EPJ Web of Conferences **160**, 05004 (2017) DOI: 10.1051/epjconf/201716005004
*Seismology of the Sun and the Distant Stars II*

# New Insights of High-precision Asteroseismology: Acoustic Radius and $\chi^2$–matching Method for Solar-like Oscillator KIC 6225718

*Tao* Wu[1,2,⋆] and *Yan* Li[1,2,⋆⋆]

[1] *Yunnan Observatories, Chinese Academy of Sciences, P.O. Box 110, Kunming 650216, China*
[2] *Key Laboratory for Structure and Evolution of Celestial Objects, Chinese Academy of Sciences, P.O. Box 110, Kunming 650216, China*

**Abstract.** Asteroseismology is a powerful tool for probing stellar interiors and determining stellar fundamental parameters. In the present work, we adopt the $\chi^2$-minimization method but only use the observed high-precision seismic observations (i.e., oscillation frequencies) to constrain theoretical models for analyzing solar-like oscillator KIC 6225718. Finally, we find the acoustic radius $\tau_0$ is the only global parameter that can be accurately measured by the $\chi^2$-matching method between observed frequencies and theoretical model calculations for a pure p-mode oscillation star. We obtain $\tau_0 = 4601.5^{+4.4}_{-8.3}$ seconds for KIC 6225718. It leads that the mass and radius of the CMMs are degenerate with each other. In addition, we find that the distribution range of acoustic radius is slightly enlarged by some extreme cases, which posses both a larger mass and a higher (or lower) metal abundance, at the lower acoustic radius end.

## 1 Introduction

Asteroseismology is a useful tool, which is usually used to determine stellar fundamental parameters, such as stellar mass, radius, surface gravity, and mean density. It is as well as used to probe the interiors of stars, such as constraining the convective overshooting of stellar convective core [1, 2] and distinguishing the status of stellar core on the red giant branches – H-shell burning stars whose center is an radiative electric degenerate He-core or He-core burning stars whose center is a convective core [3, 4].

Thanks to the space-based missions, such as *CoRoT* [5], *Kepler* [6, 7], and the following *K2* [8, 9], more and more unexpected high-precision observations have been obtained. It makes the asteroseismic researches enter the age of high-precision. In the next few years, the observation missions, such as *TESS* [10] and *PLATO 2.0* [11], will support more and more high-precision observations for the researches of asteroseismology. They will lead to the research of asteroseismology reach a new age.

In order to determine the stellar fundamental parameters and/or probe the interiors of stars, comparisons between observations and model calculations are usually used to decide the best-fitting model whose parameters and interiors will be used to characterize those of the observations [1, 2, 12–16]. The goodness of the comparison is characterized by a $\chi^2_x$-minimization method, which is defined as [17, 18]:

$$\chi^2_x = \frac{1}{N}\sum_{i=1}^{N}\frac{\left(x_i^{\rm obs} - x_i^{\rm mod}\right)^2}{\sigma^2_{x_i^{\rm obs}} + \sigma^2_{x_i^{\rm mod}}}, \quad (1)$$

where superscripts “obs" and “mod" denote the observations and model calculations, respectively. $\sigma$ and $N$ are the uncertainty of the quantity $x$ and the numbers of available quantity $x$, respectively. It is turn to

$$\chi^2_x = \frac{1}{N}\sum_{i=1}^{N}\left(\frac{x_i^{\rm obs} - x_i^{\rm mod}}{\sigma_{x_i^{\rm obs}}}\right)^2, \quad (2)$$

when $\sigma_{x_i^{\rm mod}} << \sigma_{x_i^{\rm obs}}$. Obviously, for the value of $\chi^2_x$, the smaller, the better. The theoretical model is closer to the observations.

In the present work, we will try to only use those high-precision seismic observations (i.e., oscillation frequencies $\nu_{nl}$) to analyze the theoretical calculation models. However, what can the $\chi^2_\nu$ analysis tell us about the physical information of the investigated targets? Or, in other words, what physical parameters of the investigated target can be determined best with such an analysis method? In the following, we will try to answer such question via analyzing the theoretical calculation models and the oscillation frequencies of the solar-like oscillator *KIC 6225718*.

### KIC 6225718

*KIC* 6225718 is also named HIP (HIC) 97527 and HD 187637. It is a low-mass main-sequence star [19], whose

⋆e-mail: wutao@ynao.ac.cn
⋆⋆e-mail: ly@ynao.ac.cn

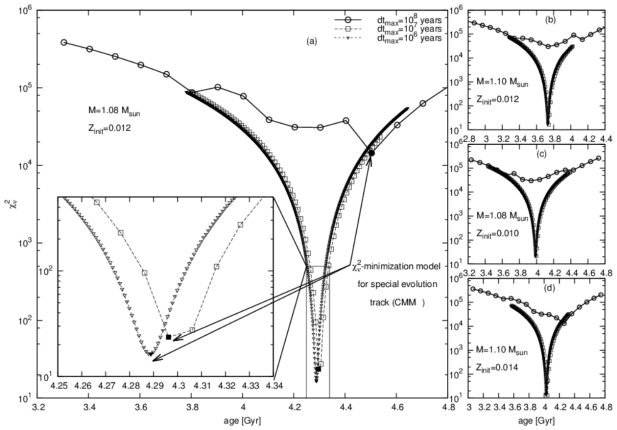


**Figure 1:** $\chi^2_\nu$ as a function of stellar age $\tau_{\rm age}$. Different panels show different masses and initial metal abundances. They are symbolled at the figure with text. In panels, different point styles represent different time step. They are about $10^8$, $10^7$, and $10^6$ years, respectively. In panel (a), filled points denote the $\chi^2_\nu$-minimization models (CMMs) [18].

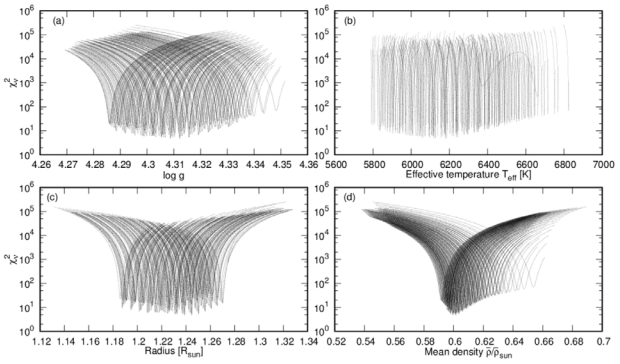


**Figure 2:** $\chi^2_\nu$ as a function of surface gravity $\log g$–panel (a), effective temperature $T_{\rm eff}$–panel (b), radius $R$–panel (c), and of mean density $\bar{\rho}$–panel (d), respectively [18].

mass ranges from 1.08 to 1.37 $M_\odot$. In addition, its metal abundance [Fe/H] ranges from −0.24 to −0.10 dex [18]. Its mass $M$ and metal abundance [Fe/H] are $1.03 - 1.52\ M_\odot$ and $-0.38 - +0.0.02$ dex, respectively, when their observational uncertainties are considered [18]. Based on the observations of *Kepler* (there are 18 long-cadence (about 30 minutes exposure time) quarters Q0-Q17 and 13 short-cadence (about 1 minute exposure time) quarters Q0 and Q6-Q17) during more than 4 years, the obvious works analyzed parts of the light curves and extracted the frequency of maximum oscillation power $\nu_{\rm max} = 2301 - 2351\ \mu$Hz and the large frequency separation $\Delta\nu \simeq 105.8\ \mu$Hz [1, 20–23]. In the present work, we use the 33 individual frequencies and their uncertainties, which is from the work of Tian et al. (2014) [1].

### Modeling

We use MESA (v6208) evolutionary code to calculate the theoretical models and their oscillation information (i.e., oscillation frequencies) [24–26]. For the stellar mass $M$ and the initial heavy element mass fraction $Z_{\rm init}$, they are $M = 1.00 - 1.26\ M_\odot$ with a step of $0.02\ M_\odot$ and $Z_{\rm init} = 0.010 - 0.036$ with a step of 0.002, respectively. For more descriptions of the physical input and other initial input parameters of the model calculations, please refer to the work of Wu & Li (2016) [18]. In order to void the influence due to the outer boundary of stellar model for oscillation frequencies, the outer boundary of stellar model is fixed at optical depth $\tau = 10^{-3}$ in our model calculations.

## 2 Results and Discussions

In calculating stellar theoretical models, the time steps (or time resolutions) will affect the precision of model. Figure 1 shows four different evolutionary tracks. For every evolutionary tracks, there are three different time steps. They are $10^8$, $10^7$, and $10^6$ years, respectively. It can be seen from Figure 1 that the stellar evolutions whose time step is $10^8$ years are fully different from those of $10^7$ years time step. For the time steps of $10^7$ and $10^6$ years, except for the latter has larger time resolution (i.e., smaller time step) to precisely decide the $\chi^2$-minimization model (CMM) for every evolutionary tracks, they are almost the same. In addition, it can be found from Figure 1 that the evolutions need larger time resolution (i.e., smaller time step), when the theoretical models are closer to the real situation of investigated target.

All of the calculated $\chi^2_\nu$ are shown in Figures 2 and 3. In the two figures, every lines represent an evolutionary tracks. In Figure 2, the $\chi^2_\nu$ as a function of surface gravity $\log g$, effective temperature $T_{\rm eff}$, radius $R$, and of mean density $\bar{\rho}$ of stars, respectively. It can be seen from Figure 2 that the profiles of $\chi^2_\nu$ are in a state of disorder not only with $\bar{\rho}$ but also with $\log g$, $T_{\rm eff}$, and $R$. Despite they are related with the frequency of the maximum oscillation power $\nu_{\rm max}$ and the large frequency separation $\Delta\nu$ with the following relations [27–29]:

$$\frac{\nu_{\rm max}}{\nu_{\rm max,\odot}} = \frac{M/M_\odot}{(R/R_\odot)^2\sqrt{T_{\rm eff}/T_{\rm eff,\odot}}} = \frac{g/g_\odot}{\sqrt{T_{\rm eff}/T_{\rm eff,\odot}}}, \quad (3)$$

and

$$\frac{\Delta\nu}{\Delta\nu_\odot} = \sqrt{\frac{M/M_\odot}{(R/R_\odot)^3}} = \sqrt{\bar{\rho}/\bar{\rho}_\odot}. \quad (4)$$

In Figure 3, however, the profiles of $\chi^2_\nu(\tau_0)$ are convergence on the acoustic radius $\tau_0$. It is defined as [30, 31]:

$$\tau_0 = \int_0^R \frac{dr}{c_{\rm s}}, \quad (5)$$

where $c_{\rm s}$ is the adiabatic sound speed. The $\chi^2_\nu(\tau_0)$ curves are close each other, even overlap. All of the calculations construct a perfect "V" shape. All the CMMs almost point the same point on acoustic radius $\tau_0$. It is about 4600 seconds. From this, we conclude that the acoustic radius $\tau_0$ is the global model parameter that can be determined best

DOI: 10.1051/epjconf/201716005004

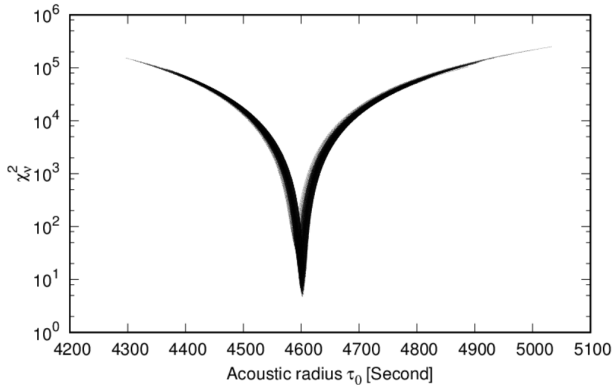


**Figure 3:** $\chi^2_\nu$ as a function of stellar acoustic radius $\tau_0$ [18].

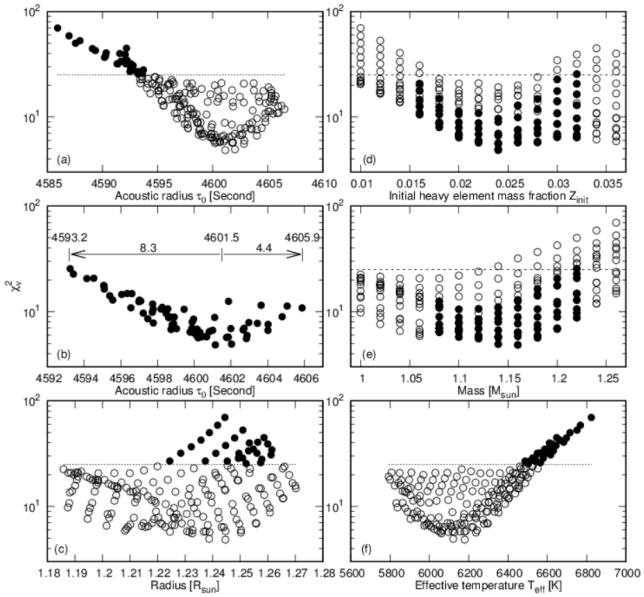


**Figure 4:** The $\chi^2_\nu$ of CMMs as a function of stellar acoustic radius $\tau_0$–panels (a) and (b), radius $R$–panel (c), initial metal abundance $Z_{\rm init}$–panel (d), mass $M$–panel (e), and of effective temperature $T_{\rm eff}$–panel (f), respectively [18]. For the filled points, panels (a) and (b) correspond to panels (c) and (f), and to panels (d) and (e), respectively.

from matching the observed frequencies with the theoretical ones. In other words, the propagation time of sound speed from stellar surface to its center can be precisely determined without any other constraint.

The distributions of CMMs ($\chi^2_{\nu,\rm CMM}$) are shown in Figure 4 against the acoustic radius $\tau_0$, radius $R$, mass $M$, initial abundance $Z_{\rm init}$, and effective temperature $T_{\rm eff}$. It can be seen from Figure 4(a) that the distribution of CMMs ($\chi^2_{\nu,\rm CMM}(\tau_0)$) looks like a ladle. They are divided into two parts with the dashed line of $\chi^2_{\nu,\rm CMM} = 25$. Most of the CMMs are located in the bowl-shape part ($\chi^2_{\nu,\rm CMM} < 25$) and the rest form the handle ($\chi^2_{\nu,\rm CMM} > 25$). It can be seen from Figures 4(d)-(e) that the minimum of $\chi^2_{\nu,\rm CMM}$ is realized by stellar models with $Z_{\rm init} = 0.024$, and $M = 1.14\ M_\odot$ and $1.16\ M_\odot$. The CMMs whose $1.08 \le M \le 1.22\ M_\odot$, and $0.016 \le Z_{\rm init} \le 0.032$ occupy the center part

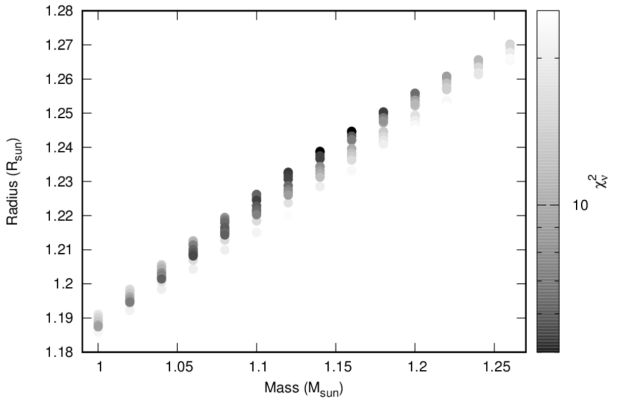


**Figure 5:** The radius $R$ of CMMs as a function of their masses $M$.

in Figures 4(d)-(e). They from the lower edge of the ladle (see Figure 4(b)). It can be found from Figure 4(b) that the acoustic radius of KIC 6225718 can be determined as $\tau_0 = 4601.5^{+4.4}_{-8.3}$ seconds.

It can be found from Figures 4(a), (d)-(e) that the outlying part (handle part) has larger mass $M$ and smaller or higher metal abundance $Z_{\rm init}$ comparing with the normal part (bowl-shape part). The outlying part has smaller acoustic radius $\tau_0$ (see Figure 4(a)) than the normal part. It is due to the increase of stellar radius $R$ (see Figure 4(c)) can not offset the increase of adiabatic sound speed $c_{\rm s}(r)$, i.e., temperature $T(r)$ (see Figure 4(f)). From this, we conclude that the larger stellar mass and higher or lower metal abundance slightly affect the distribution of $\chi^2_{\nu,\rm CMM}(\tau_0)$. It leads that the CMMs have smaller acoustic radius.

The distribution of $R(M)$ for all of the calculated CMMs are shown in Figure 5. It can be seen from Figure 5 that those CMMs are located in a narrow band. They are close each other and almost can not be clearly distinguished. In other words, the stellar mass is degenerate with its radius for those CMMs. In the theory of stellar oscillation, the acoustic radius $\tau_0$ is related with the stellar mass $M$ and radius $R$ with the relation of $\tau_0 \sim (M/R^3)^{-1/2}$ [30, 31]. While, the above analysis indicates that, for a given star, the acoustic radius of CMMs can be roughly referred as a constant. Therefore, we obtain the relation: $(M/R^3)^{-1/2} \simeq const.$. The stellar mass of CMMs vary with its radius $M \sim R^3$.

## 3 Conclusions

In the present work, we only use the high-precision asteroseismic observations (i.e., oscillation frequencies) to constrain the theoretical models with the method of $\chi^2_\nu$-matching to analyze the solar-like oscillator KIC 6225718. On the other hands, we consider the influence of the model precision for deciding the CMM and set its time step as $10^6$ years. Finally, we find that the acoustic radius $\tau_0$ is the global parameters that can be determined best from matching the observed frequencies with the theoretical ones via the method of $\chi^2_\nu$. It is about $\tau_0 = 4601.5^{+4.4}_{-8.3}$ seconds. The

calculations suggest that the distribution of acoustic radius is slightly affected by larger stellar mass, and higher or lower metal abundance at the direction of smaller values. In addition, the approximate same $\tau_0$ leads that the mass and radius of CMMs are degenerate with each other.

### Acknowledgements

This work is cosponsored by the NSFC of China (grant Nos. 11333006, 11503076, and 11521303), and by the Chinese Academy of Sciences (grant No. XDB09010202). The authors express their sincere thanks to NASA and the Kepler team for allowing them to work with and analyze the Kepler data making this work possible and also gratefully acknowledge the computing time granted by the Yunnan Observatories.

## References

[1] Tian, Z. J., et al., MNRAS, 445, 2999 (2014)
[2] Moravveji, E., et al., A&A, 580, A27 (2015)
[3] Bedding, T. R., et al., Nature, 471, 608 (2011)
[4] Mosser, B., et al., A&A, 572, 5 (2014)
[5] Baglin, A., et al., in COSPAR, Plenary Meeting, Vol. 36, 36th COSPAR Scientific Assembly, 3749 (2006)
[6] Gilliland, R. L., et al., PASP, 122, 131 (2010)
[7] Koch, D. G., et al., ApJL, 713, L79 (2010)
[8] Haas, M. R., et al., American Astronomical Society Meeting Abstracts #223, 223, #228.01 (2014)
[9] Howell, S. B., et al., PASP, 126, 398 (2014)
[10] Ricker, G. R., et al., Bulletin of the American Astronomical Society, 41, 403.01 (2009)
[11] Catala, C., et al., Pathways Towards Habitable Planets, 430, 260 (2010)
[12] Guenther, D. B., & Brown, K. I. T., ApJ, 600, 419 (2004)
[13] Lebreton, Y., Progress in Solar/Stellar Physics with Helio- and Asteroseismology, 462, 469 (2012)
[14] Lebreton, Y., & Goupil, M. J., A&A, 569, A21 (2014)
[15] Roxburgh, I. W., & Vorontsov, S. V., A&A, 560, A2 (2013)
[16] Roxburgh, I. W., A&A, 585, A63 (2016)
[17] Eggenberger, P., et al., A&A, 417, 235 (2004)
[18] Wu, T., & Li, Y., ApJL, 818, L13 (2016)
[19] Boyajian, T. S., et al., ApJ, 771, 40 (2013)
[20] Bruntt, H., et al., MNRAS, 423, 122 (2012)
[21] Chaplin, W. J., et al., ApJS, 210, 1 (2014)
[22] Huber, D., et al., ApJ, 760, 32 (2012)
[23] Silva Aguirre, V., et al., ApJ, 757, 99 (2012)
[24] Paxton, B., et al., ApJS, 192, 3 (2011)
[25] Paxton, B., et al., ApJS, 208, 4 (2013)
[26] Christensen-Dalsgaard, J., Ap&SS, 316, 113 (2008)
[27] Brown, T. M., et al., ApJ, 368, 599 (1991)
[28] Belkacem, K., et al., A&A, 530, A142 (2011)
[29] Kjeldsen, H., & Bedding, T. R., A&A, 293, 87 (1995)
[30] Christensen-Dalsgaard, J., Lecture Notes on Stellar Oscillations, Aarhus University, (2003)
[31] Aerts, C., Christensen-Dalsgaard, J., & Kurtz, D. W., Asteroseismology (Astronomy and Astrophysics Library; Dordrecht: Springer Science+Business Media B.V.), 207 (2010)